Synthetic paramontroseite VO_2 with good aqueous lithium–ion battery performance†

Changzheng Wu, Zhenpeng Hu, Wei Wang, Miao Zhang, Jinlong Yang and Yi Xie*

Received (in Cambridge, UK) 9th April 2008, Accepted 16th May 2008
First published as an Advance Article on the web 26th June 2008
DOI: 10.1039/b806009f

Synthetic paramontroseite VO_2 has been successfully obtained using a simple chemical reaction route for the first time after fifty years; the paramontroseite phase shows a conducting property and good aqueous lithium ion battery performance.

In the 1950s, Mrose and Evans discovered a new mineral paramontroseite VO_2 from the Colorado Plateaus region.[1] Paramontroseite vanadium dioxide (VO_2) possesses a regular tunnel form, in which the VO_6 octahedra are linked into double chains and the double chains link corners with each other in turn to form a framework having tunnels with rectangular-shaped cross sections that are 1×2 octahedra on a side.[2,3] For more than fifty years, efforts have been strongly focused on the structural analysis of paramontroseite and the transformation relationship between paramontroseite and montroseite, owing to its fascinating tunnelled structure.[1–3] However, almost all of the experimental data for paramontroseite originated from investigation of mineral samples, and not synthetic samples. Here, we highlight an available pathway to accomplish this challenge by a simple reaction of sodium orthovanadate ($Na_3VO_4{\cdot}12H_2O$) and thioacetamide (TAA).

The fascination for paramontroseite VO_2 also arises from its structural analysis and calculation results, which indicate potentially conducting behavior. For the paramontroseite VO_2 phase, due to the presence of infinite chains along the *c*-axis with nearest V–V distances of 0.293 nm, its d-orbital electrons would be shared by all of the metal V atoms along the paramontroseite *c*-axis similar to that in tetragonal rutile VO_2 [4] (see ESI,† S1). Therefore, paramontroseite would appear to have promising electrical conducting properties at room temperature from the structural point of view. Here, first-principle calculations using the VASP program were also performed to further understand the conducting behavior of paramontroseite VO_2, and the spin-dependent density of states (DOS) and energy bands of paramontroseite VO_2 are shown in Fig. 1. In Fig. 1(b), the DOS resides across the Fermi level and gives a certain local DOS value at the Fermi level, indicating its metallic character. In more detail, the total DOS value of paramontroseite VO_2 around the Fermi level is mainly contributed from the V 3d and O 2p orbitals as shown in Fig. 1(b). Further, the paramontroseite phase shows a continuous DOS starting from −0.93 eV and the Fermi level tangles with its conducting bands for all the high-symmetry points (see ESI,† S2). Comparing these calculation results with those for rutile and monoclinic VO_2, it is found that the DOS of rutile VO_2 also possesses a continuous DOS around the Fermi level while the DOS of monoclinic VO_2 has a 0.1 eV wide deep minimum just above ε_F with a separated band.[5] Therefore, the characteristics of DOS and energy bands for paramontroseite VO_2 are quite similar to those of the metallic rutile VO_2 phase, rather than that of the semiconducting monoclinic VO_2 phase. This similarity of calculation results between the paramontroseite VO_2 and metallic rutile VO_2 phase thus provides further evidence for the metallic behavior of the paramontroseite VO_2 structure.

Moreover, as observed from the DOS and energy bands for paramontroseite VO_2 (see ESI,† S2), it can be seen that the one spin direction (spin up) behaves like a metal and the other (spin down) is semiconducting, showing the half-metal property with a complete polarization of electrons at the Fermi level. That is to say, paramontroseite VO_2 in orthorhombic structure is also amenable to spintronics and spin injection.[6]

Our experimental results show that the paramontroseite VO_2 could be chemically synthesized by a simple reaction of sodium orthovanadate ($Na_3VO_4{\cdot}12H_2O$) and thioacetamide (TAA). Details of the experimental process can be described as follows: first, 4 mmol $Na_3VO_4{\cdot}12H_2O$ and 20 mmol thioacetamide (TAA) were dissolved in 50 ml distilled water to form a homogeneous solution in a glass jar. This solution was then loaded into a 50 ml Teflon-lined autoclave, which was sealed and heated at 220 °C for 10 h. The system was then allowed to

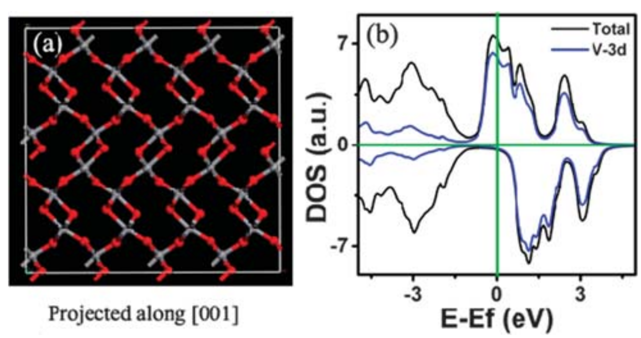

Fig. 1 (a) The supercell model of orthorhombic paramontroseite VO_2 projected along [001]. (b) Spin-dependent density of states. The black line shows the total DOS, the blue lines the V 3d partial DOS.

Hefei National Laboratory for Physical Sciences at Microscale, University of Science and Technology of China, Hefei, 230026, P. R. China. E-mail: yxie@ustc.edu.cn; Fax: 86-551-3603987

† Electronic supplementary information (ESI) available: Structural analysis, band gap, experimental details, morphology, SAED pattern and XPS analysis of the sample. See DOI: 10.1039/b806009f

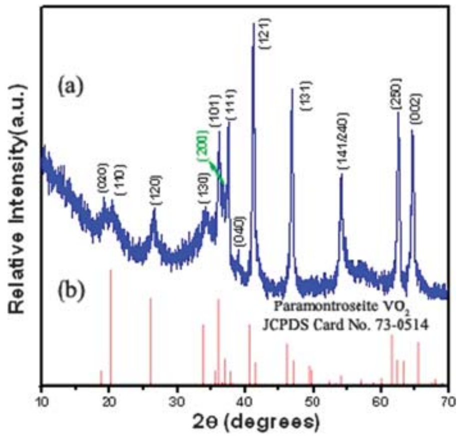

Fig. 2 XRD pattern for the paramontroseite VO_2.

cool to room temperature. The final product was collected by centrifugation, and washed with deionized water and ethanol to remove any possible ionic remnants, and then dried in vacuum at 60 °C.

The XRD pattern of the as-obtained product could readily be indexed to orthorhombic paramontroseite VO_2 with the cell parameters a = 4.956 Å, b = 9.332 Å and c = 2.896 Å, as shown in Fig. 2.‡ Further evidence for the presence of paramontroseite VO_2 comes from a high-resolution TEM image (HRTEM) and selected area electron diffraction (SAED) pattern (Fig. 3). Since paramontroseite VO_2 exhibits a walnut-like morphology according to the panoramic FE-SEM image (see ESI,† S4), the HRTEM images and its corresponding SAEDs were performed on the edges of the typical VO_2 walnut-like architectures as shown in Fig. 3. The interplanar distances of 2.50, 2.45, 4.68, 1.69 Å match well with the d_{101}, d_{200}, d_{020}, d_{240} spacings, respectively, of paramontroseite VO_2. Moreover, based on the careful calculations for the angle values of each lattice plane in the same SAED pattern, it is found that all the orientation angle values of these planes appeared in the SAED patterns were fairly consistent with those calculated from orthorhombic crystallographic parameters of paramontroseite VO_2 (see ESI,† S5), which provided further clear evidence for the formation of crystallographic paramontroseite in the as-obtained sample.

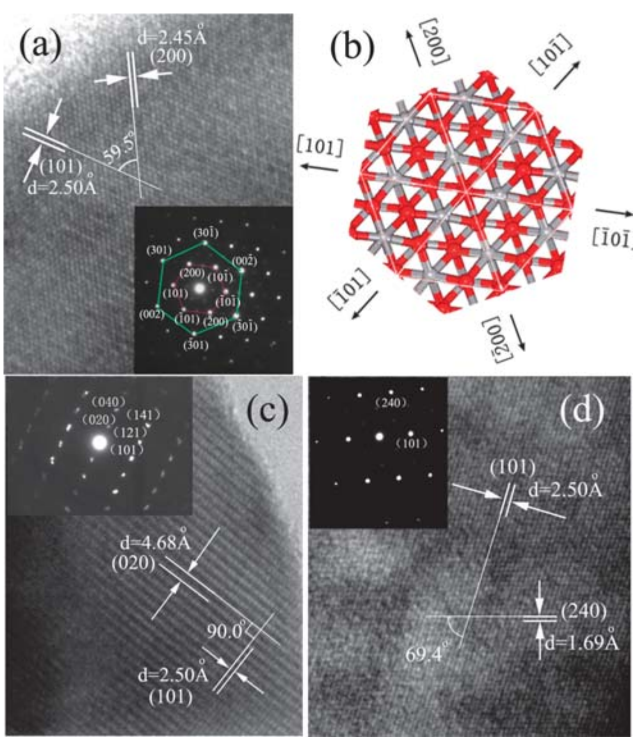

Fig. 3 High-resolution TEM image and selected electron diffraction patterns on the edge of a typical paramontroseite VO_2 walnut-like architecture. (b) Approximate hexagonal atomic arrangement in the paramontroseite crystal structure when projected along the b-axis, further conforming the as-obtained product was paramontroseite VO_2.

Of note, the crystal structure of paramontroseite VO_2 as shown in Fig. 3(b) reveals a unique approximate-hexagonal atomic arrangement when projected along the b-axis direction. Such approximate-hexagonal symmetry had already been theoretically recognized in Mader's calculated ED pattern.[7] Our experimental ED pattern shown in Fig. 3(a) also gives the approximate-hexagonal characteristic and the crystallographic plane indexes agrees well with those in the calculated ED pattern, which provided further diagnostic and direct evidence for the paramontroseite phase.

The room-temperature conductivity of the as-obtained paramontroseite VO_2 was measured to be 1.02 S cm^{-1}, showing higher conductivity than many other inorganic conducting materials.[8–10]

The as-obtained conducting paramontroseite VO_2 walnut-like nanoarchitectures should thus facilitate the intercalation/deintercalation of lithium ions in lithium ion batteries (LIBs) due to the high electrical conductivity and the increased diffusion coefficient within the nanoarchitectures.[11,12] The tunnel size (4.946 Å × 2.851 Å) in the supercell crystal structure of paramontroseite VO_2 is considerably larger than the diameter of Li ion (1.36 Å). Obviously, the presence of the tunnels in paramontroseite VO_2 could be effective in facilitating Li-ion diffusion through the crystal structure, so facilitating the electrochemical reaction, which should contribute the Li-ion insertion performance in the Li-ion battery. Bearing in mind that the above advantage of paramontroseite VO_2, here, we introduced paramontroseite VO_2 as the active material for aqueous lithium ion battery applications, on the consideration that the development of an aqueous solution as electrolyte in rechargeable lithium-ion batteries was an effective way to realize a highly desirable[13] safer and less-expensive battery by replacement of organic electrolyte.

The discharge curves of the paramontroseite $VO_2/LiMn_2O_4$ aqueous LIB (5 M $LiNO_3$ and 0.001 M LiOH) are shown in Fig. 4(a) which displays the 1st, 2nd, 20th and 50th cycle of the cell with cutoff voltages of 1.70 and 0.5 V at a current density of 60 mA g^{-1}.

It can be clearly found that the paramontroseite VO_2 electrode promotes the electrochemical performance in aqueous LIBs. First, the paramontroseite VO_2 electrode shows both discharge capacity and the output voltage advantages in our aqueous LIBs, revealing the high energy density of the paramontroseite $VO_2/LiMn_2O_4$ cell. The first discharge capacity of the VO_2 electrode in our paramontroseite

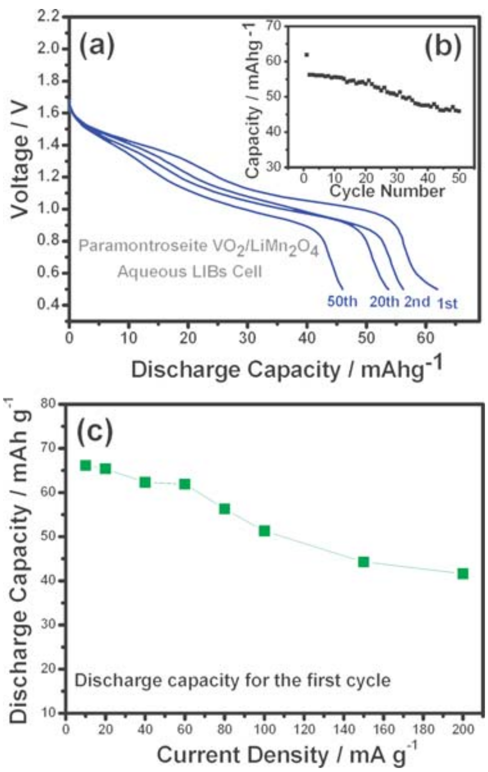

Fig. 4 (a) Voltage *vs.* discharge capacity curves for paramontroseite VO_2 electrode in aqueous 5 M $LiNO_3$ and 0.001 M LiOH as electrolyte for the 1st, 2nd, 20th and 50th cycle. The inset (b) in (a) is the cycling behavior of the paramontroseite $VO_2/LiMn_2O_4$ aqueous cell. (c) The first discharge capacity at different current densities.

$VO_2/LiMn_2O_4$ aqueous cell is 61.9 mAh g^{-1}, which is a highly significant value for aqueous LIB systems in the light of previous reports,[14–16] although it is still smaller than that in the organic electrolytes (usually >120 mA h g^{-1}).[17] Furthermore, the first output voltage of this aqueous LIB is in the range of 1.3–1.6 V, while the second average output voltage is 1.0–1.2 V. Here, the output voltage is again very impressive when compared with previous aqueous LIBs.[14–16] Also, the first output voltage for paramontroseite $VO_2/LiMn_2O_4$ aqueous LIB is higher than the output voltage of primary Zn–MnO_2, Ni–MH and Ni–Cd cell systems (*ca.* 1.2 V), while even the lowest output voltage approached 1.2 V. The relatively high output voltage and high discharge capacity value infer that our aqueous LIB is the promising substitute candidate for cells with higher energy density.

Second, it is clear that the as-obtained paramontroseite VO_2 electrode exhibits better cycling behavior than those in the previously reported aqueous LIBs.[14–16] Fig. 4(b) (inset in (a)) shows the cycling behavior at a current density of 60 mA g^{-1} between 0.5 and 1.7 V in aqueous electrolyte. It is found that the discharge capacity after 50 cycles is 45.96 mAh g^{-1}, which is approximately 74% of the first discharge capacity, while it shows good resistance to fading up to 50 cycles. Third, the paramontroseite VO_2 electrode exhibits a good stability at high current density as shown in Fig. 4(c), showing the relatively high-rate performance of this electrode, which resulted from the mitigation of kinetic limitations by the high electronic conductivity of paramontroseite VO_2.

In conclusion, synthetic paramontroseite VO_2 has been successfully obtained in this work by a simple chemical reaction route after more than 50 years; previously the chemical and physical information of paramontroseite only came from mineral samples. Both structural analysis and the first-principle calculations reveal the conducting property of paramontroseite VO_2 and experiments confirm its good conductivity. The as-obtained paramontroseite sample shows the fascinating characteristics of tunnelled crystal structure, nanoarchitectured morphology and its conducting property, which entail superior aqueous LIB performance in the $VO_2/LiMn_2O_4$ aqueous LIB system. Compared with previous aqueous LIBs, the paramontroseite $VO_2/LiMn_2O_4$ cell exhibits high energy density, better cycling behavior and high-rate capability, which is of great use for potential industrial applications.

This work was financially supported by the National Natural Science Foundation of China (No. 20621061) and the China Postdoctoral Science Foundation.

Notes and references

‡ The sample was characterized by X-ray powder diffraction (XRD) with a Philips X'Pert Pro Super diffractometer with Cu-K_α radiation (λ = 1.54178 Å). The field emission scanning electron microscopy (FE-SEM) images were taken on a JEOL JSM-6700F SEM. The transmission electron microscopy (TEM) images were carried out on a JEOL-2010 TEM at an acceleration voltage of 200 kV. The electrical conductivity of the as-prepared paramontroseite VO_2 was measured with the use of a computer-controlled, four-probe technique.

1 H. T. Evans, Jr and M. E. Mrose, *Am. Mineral.*, 1955, **40**, 861.
2 B. G. Hyde, A. N. Bagshaw, S. Anderson and M. O. Keeffe, *Annu. Rev. Mater. Sci.*, 1974, **4**, 43.
3 L. Löffler and W. Mader, *J. Am. Ceram. Soc.*, 2003, **86**, 534.
4 Ch. Leroux, G. Nihoul and G. Van Tendeloo, *Phys. Rev. B: Condens. Matter*, 1998, **57**, 5111.
5 K. Hermann, A. Chakrabarti, A. Haras, M. Witko and B. Tepper, *Phys. Status Solidi A*, 2001, **187**, 137–149.
6 S. Sanna, B. Hourahine, U. Gerstmann and Th. Frauenheim, *Phys. Rev. B: Condens. Matter*, 2007, **76**, 155128–155140.
7 L. Löffler and W. Mader, *J. Am. Ceram. Soc.*, 2003, **86**, 534.
8 G. Thomas, *Nature*, 1997, **389**, 907.
9 H. Kawazoe, M. Yasukawa, H. Hyodo, M. Kurita, H. Yanagi and H. Hosono, *Nature*, 1997, **389**, 939.
10 F. Q. Huang, P. Brazis, C. R. Kannewurf and J. A. Ibers, *J. Am. Chem. Soc.*, 2000, **122**, 80–86.
11 X. Wang, X. Y. Chen, L. S. Gao, H. G. Zheng, Z. D. Zhang and Y. T. Qian, *J. Phys. Chem. B*, 2004, **108**, 16401.
12 C. Z. Wu, Y. Xie, L. Y. Lei, S. Q. Hu and C. Z. Ouyang, *Adv. Mater.*, 2006, **18**, 1727.
13 A. N. Jansen, A. J. Kahaian, K. D. Kepler, P. A. Nelson, K. Amine, D. W. Dees, D. R. Vissers and M. M. Thackeray, *J. Power Sources*, 1999, **81–82**, 902.
14 G. James, *Science*, 1994, **264**, 1084.
15 J. Kohler, H. Makihara, H. Uegaito, H. Inoue and M. Toki, *Electrochim. Acta*, 2000, **46**, 59.
16 G. J. Wang, L. Fu, N. H. Zhao, L. C. Yang, Y. P. Wu and H. Q. Wu, *Angew. Chem., Int. Ed.*, 2007, **46**, 295; G. J. Wang, L. Fu, N. H. Zhao, L. C. Yang, Y. P. Wu and H. Q. Wu, *Angew. Chem.*, 2007, **119**, 299.
17 M. Okubo, E. Hosono, J. Kim, M. Enomoto, N. Kojima, T. Kudo, H. Zhou and I. Honma, *J. Am. Chem. Soc.*, 2007, **129**, 7444–7452.